Tectonophysics 471 (2009) 216–224

Contents lists available at ScienceDirect

Tectonophysics

journal homepage: www.elsevier.com/locate/tecto

Brittle deformation relating to the Carboniferous–Cretaceous evolution of the Lambert Graben, East Antarctica: A precursor for Cenozoic relief development in an intraplate and glaciated region

G. Phillips [a,b,*], A.L. Läufer [c]

[a] The University of Newcastle, Discipline of Earth Sciences, Newcastle, New South Wales, 2308, Australia
[b] School of Earth Sciences, The University of Melbourne, Parkville, Victoria, 3010, Australia
[c] Bundesanstalt für Geowissenschaften und Rohstoffe, Hannover, Germany

ARTICLE INFO

Article history:
Received 13 October 2008
Received in revised form 11 February 2009
Accepted 12 February 2009
Available online 24 February 2009

Keywords:
East Antarctica
Gamburtsev Mountains
Lambert Graben
Palaeostress
Intracontinental relief
Stress inversion

ABSTRACT

Stress inversions of kinematic data measured from brittle deformation structures exposed in the southern Prince Charles Mountains have been carried out to elucidate the drivers of intracontinental deformation responsible for the development of the Lambert Graben, East Antarctica. Four palaeostress fields (*D*1–*D*4) were identified from these data, which when coupled with pre-existing geochronological and sedimentological evidence, provide a clear deformation framework. The architecture of the Lambert Graben is dominantly defined by north–south trending *D*2 and northeast–southwest trending *D*3 faults that formed respectively during: (1) Carboniferous–Permian intracontinental extrusion and (2) Cretaceous transtensional tectonics related to the dispersion of East Gondwana. Interestingly, sub-ice topography in the southern Prince Charles Mountains and further south towards the Gamburtsev Mountains is defined by bedrock lineaments that parallel the orientations of the main fault arrays. Previous work shows that the development of relief in the southern Prince Charles Mountains is Tertiary in age and probably not associated with Carboniferous–Permian or Cretaceous tectonic events. Based on a clear spatial link between the orientations of faults and bedrock lineaments, we suggest that inherited fault zones were integral in accommodating uplift driven by plate flexure as a response to crustal unloading during glacial incision.

1. Introduction

The Lambert Graben in East Antarctica is considered to represent a failed rift system that formed in central East Gondwana during the Carboniferous to Cretaceous (Fig. 1; Powell et al., 1988; Lisker et al., 2003; Boger and Wilson, 2003). The timing and processes associated with the development of this graben are topics of considerable debate, which is dictated by conflicting interpretations drawn from geophysical, geochronological, sedimentological and structural data (Tewari and Veevers, 1993; Arne, 1994; McLoughlin and Drinnan, 1997a,b; Mishra et al., 1999; Lisker et al., 2003; Boger and Wilson, 2003; Harrowfield et al., 2005). For example, a correlation between the timing of basement denudation (apatite fission track data; Arne, 1994; Lisker et al., 2003) and sediment deposition (palynological data; McLoughlin and Drinnan, 1997a,b) has been used to suggest that the graben formed during two distinct stages; the first in the Carboniferous–Permian and the second in the early Cretaceous (Lisker et al., 2003). Conversely, a palaeostress analysis of kinematic data from brittle deformation structures revealed a single uniform stress field, which supports a single-stage tectonic model (Boger and Wilson, 2003). To resolve these ambiguities, a model that encompasses all of the available geophysical, geochronological, sedimentological and structural data is required.

Based on the aforementioned uncertainties, competing hypotheses for the manifestation of intracontinental deformation in East Antarctica are presently invoked:

1. A two-stage tectonic model where: (i) intracontinental extrusion during the Carboniferous–Permian was driven by convergence along the Palaeo-Pacific margin of East Gondwana, followed by (ii) transtension during the Cretaceous that coincided with the dispersion of India and East Antarctica (Fig. 1; Lisker et al., 2003).
2. A single-stage tectonic model where: (i) uplift and denudation during the Permian was passive in nature and related to the development of intracontinental sag basins associated with erosion and distribution of sediment way from an intracontinental highland (Tewari and Veevers, 1993), followed by (ii) the development of the Lambert Graben during a single phase of transtension that coincided with the dispersion of India and East Antarctica during the early Cretaceous (Boger and Wilson, 2003).

As a result of these two models, our understanding of intracontinental tectonics in central East Gondwana during the Carboniferous to Cretaceous is unclear.

* Corresponding author. The University of Newcastle, Discipline of Earth Sciences, Newcastle, New South Wales, 2308, Australia. Tel.: +61 2 4921 5410; fax: +61 02 4921 6925.
E-mail address: Glen.Phillips@newcastle.edu.au (G. Phillips).

0040-1951/$ – see front matter
doi:10.1016/j.tecto.2009.02.012

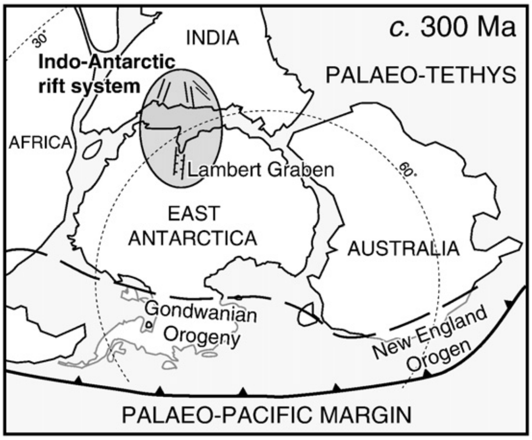

Fig. 1. Map of East Gondwana at c. 300 Ma (after Tewari and Veevers, 1993 and Lisker et al., 2003) showing the location of the Indo–Antarctic rift system. The focus of this study is the Lambert Graben. Locations of the New England Orogen in Australia and Gondwanian Orogen in Antarctica are shown.

In this paper, we present the results of stress inversions carried out on kinematic data measured from brittle–ductile and brittle deformation features exposed in the southern Prince Charles Mountains of East Antarctica (Fig. 2). These mountains are exposed along the shoulders of the Lambert Graben and preserve a complex record of brittle–ductile to brittle deformation structures (Mishra et al., 1999; Läufer and Phillips, 2007). Inversion of kinematic data collected from these structures provides a record of ancient stress fields responsible for upper crustal deformation, which in turn, can be used to elucidate the tectonic drivers of graben development. To assimilate these data with current geodynamic models for East Antarctica, the palaeostress framework constructed from this study is tested against pre-existing geochronological, sedimentological and structural data (Arne, 1994; McLoughlin and Drinnan, 1997a,b; Lisker et al., 2003; Boger and Wilson, 2003).

In addition to providing valuable insights into the timing and nature of intracontinental deformation in East Gondwana, this study has also revealed a potential relationship between inherited tectonic structures and geomorphologically controlled relief development in an intracontinental region. High-resolution ice radar data from the southern Prince Charles Mountains and Gamburtsev Mountains (Fig. 2) indicate that bedrock topography is primarily delineated by north, northeast and east–northeast orientated linear escarpments (Damm, 2007). A comparison between the orientation of these lineaments and brittle deformation structures in the Lambert Graben region reveals a clear spatial link. Based on this correlation, we discuss the potential importance of inherited tectonic structures on the development of relief in glaciated, intracontinental regions.

2. Background geology

2.1. Basement and rift geology

In the southern Prince Charles Mountains, the Lambert Graben overprints deformed metamorphic rocks of the Lambert and Tingey Complexes (Fig. 2; Kamenev et al., 1993; Phillips et al., 2006; Corvino et al., 2007). The Lambert Complex consists of multiply deformed amphibolite to granulite rocks that were metamorphosed during the early Neoproterozoic Rayner Orogenic event (Tingey, 1991; Corvino et al., 2008). Rocks of the Tingey Complex (or Ruker Complex of Boger et al., 2006) record structural, metamorphic and geochronological evidence for a complex Archaean–Palaeozoic tectonothermal history (Mikhalsky et al., 2001; Boger et al., 2006; Phillips et al., 2006, 2007; Boger et al., 2006, 2008). As part of this history, deposition of the Sodruzhestvo Group occurred during the Neoproterozic (Fig. 2; Phillips et al., 2006).

The Lambert Graben is interpreted as a failed rift that extends approximately 700 km from Prydz Bay towards the Antarctic interior (Fig. 2; Federov et al., 1982; Mishra et al., 1999). It narrows from 300 km in Prydz Bay to approximately 20 km in the southern Prince Charles Mountains (Federov et al., 1982; Damm, 2007). The thickness of continental crust in the central part of the graben is estimated to be between 22 and 24 km (Federov et al., 1982). The graben is infilled by a succession of late Palaeozoic to Mesozoic siliciclastic sediments that are exposed, in part, as the Amery Group in the northern Prince Charles Mountains (Fig. 2). Deposition of the Amery Group occurred between 300 and 240 Ma and comprises a succession of conglomerates overlain by packages of sandstone, coal and mudstone (McLoughlin and Drinnan, 1997a,b). The thickness of this incomplete section is 2 km and is in faulted contact with metamorphic rocks of Proterozoic basement. In offshore Prydz Bay, sediments deposited during the early Cretaceous to Cenozoic overlie sedimentary rocks of probable Permian age (Turner and Padley, 1991). In total, an approximate thickness of 6–7 km of Palaeozoic-Mesozoic sediments are interpreted to infill the Lambert Graben (Mishra et al., 1999).

The timing of crustal deformation related to graben development is potentially constrained by the available mafic and felsic dyke geochronology and apatite fission track data. Whole rock K-Ar dating of diorite dykes yield ages of 245 ± 11 Ma and 239 ± 12 Ma, which is in accord with a biotite K-Ar date of 246 ± 6 Ma from an alkaline basalt

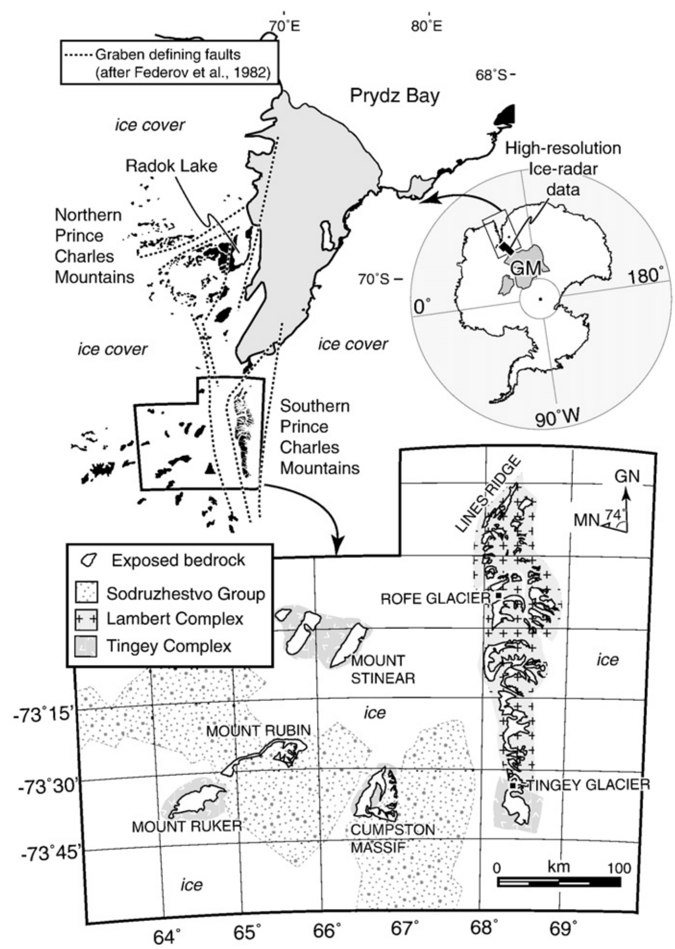

Fig. 2. Locality and geological maps of the Lambert Graben region (after Federov et al., 1982; Mikhalsky et al., 2001) and southern Prince Charles Mountains (Mikhalsky et al., 2001; Phillips et al., 2006; McLean et al., 2008). Outline of Sodruzhestvo Group is defined by geophysical methods as explained in McLean et al. (2008). GM — Gamburtsev Mountains.

sill (Sheraton, 1983; Hofmann, 1991). K-Ar dating of phlogopite in lamprophyres indicates that emplacement occurred at 110 ± 3 Ma (Walker and Mond, 1971), which is comparable to K-Ar whole rock ages for mafic dykes between 132 ± 9 and 103 ± 5 Ma (Hofmann, 1991). Rb-Sr and K-Ar whole rock analyses also indicate the emplacement of sparse alkaline dykes between 50 and 40 Ma (Tingey, 1991; Andronikov et al., 1998). Apatite fission track studies from the region also define two predominant populations of age data, the first during the Carboniferous–Triassic and the second during the early Cretaceous (Arne, 1994; Lisker et al., 2003, 2007).

Based on structural overprinting relationships, at least three generations of brittle deformation have been identified in the southern Prince Charles Mountains (Läufer and Phillips, 2007). D1 structures are brittle–ductile reverse high-strain zones with cogenetic extension veins, semi-brittle reverse faults coated with muscovite, biotite and chlorite, and bedding plane flexural slip. D1 structures generally strike north–northwest and south–southeast and dip moderate to steeply to the west–southwest. *D*2 structures are brittle in nature and formed as north–south to northeast–southwest trending normal faults and east–west trending conjugate faults. Fibres of quartz and calcite coat the *D*2 fault planes. The youngest structures (*D*3) are late-stage faults that consistently offset or reactivate the *D*1 and *D*2 structures. The predominant orientation of *D*3 faults is east–west to northwest–southeast with fault surfaces either coated with calcite fibres or quartz.

2.2. Physiography

The Mawson Escarpment dominates the topography of the southern Prince Charles Mountains (Fig. 2). Bordering the western margin of the Mawson Escarpment is the world's largest ice-stream, the Lambert Glacier, which is responsible for draining approximately one-fifth of the East Antarctic Ice Sheet into the Southern Ocean each year. To the west of the Lambert Glacier are sporadically exposed nunataks and ranges that are dominated by the peaks of Mounts Stinear (~2000 m above sea level (masl)), Rubin (~1900 masl) and Ruker (~1600 masl) and Cumpston Massif (~1650 masl). These escarpments and nunataks largely comprise two distinct morphologies, namely: 1) flat-topped benches defined by steeply sloping escarpments, or 2) rounded dome-like morphologies covered by thick moraine fields. Characteristic of the flat-topped bench morphology is a planar pre-Oligocene erosional surface that is thought to be fluvial in nature (Bardin, 1977; Wellman and Tingey, 1981). This land surface is at a similar altitude across geographically separated nunataks and is, therefore, interpreted to have been contiguous prior to the Oligocene.

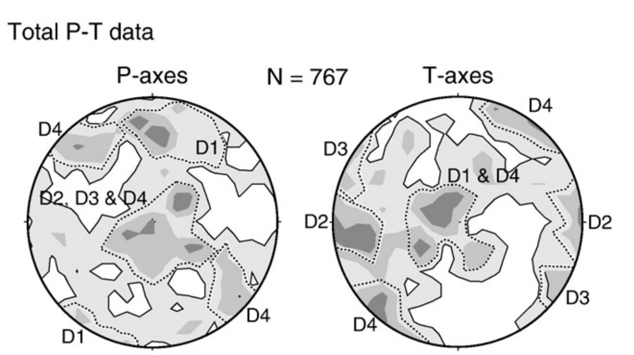

Fig. 3. Contour plot of *P*-axes (σ1) and *T*-axes (σ3) from the total dataset showing populations of stress tensors associated with each deformation event. Plot is a 2% Kamb contour plot with significance level of 3.0. Four main homogeneous populations of kinematic data can be separated from the total data.

3. Stress inversion of kinematic data

3.1. Methods

The inversion of a large kinematic data set ($n = 767$) collected from the southern Prince Charles Mountains provides a unique opportunity to elucidate the dynamic evolution of the Lambert Graben (Läufer and Phillips, 2007; Phillips, 2007). Data was collected from six locations: (1) Rofe Glacier; (2) Tingey Glacier; (3) Cumpston Massif; (4) Mount Ruker; (5) Mount Rubin, and; (6) Mount Stinear (Fig. 2). From the kinematic data, palaeostress fields were calculated using the stress inversion techniques of Angelier and Mechler (1977) and Angelier (1979). This technique employs the fault plane orientation, the azimuth of slip (transport direction) and knowledge of the sense of transport to determine the stress tensor responsible for faulting (Angelier, 1979). To identify homogenous populations of stress tensors within the large database, the *P*–*T* approach of Turner (1953) and Marrett and Allmendinger (1990) was used. This approach represents kinematic data from each fault as a pressure (*P* or σ_1) and tension (*T* or σ_3) axis. Calculation, plotting and contouring (Kamb Contour-interval = 2.0, significance level = 3.0) of *P*–*T* axes were carried out using the software package Faultkin v.4.3.5 (Allmendinger et al., 1992).

To elucidate palaeostress fields attributable to the main deformation events, the following approach was taken: (1) *P*-axis and *T*-axis for each measured fault were calculated (Fig. 3); (2) stress tensors from faults of known *D*1, *D*2 or *D*3 origin were determined to provide an approximate tensor for each event (for this step, faults were selected on the basis that they could be clearly related to *D*1, *D*2 or *D*3 and were formed by far-field stress, that is, distal to contacts between units comprising vastly different rheologies or proximal to pre-existing fault zones and anisotropies such as bedding or foliation); (3) stress tensors from the total dataset were then separated into populations related to *D*1, *D*2 or *D*3 events (Fig. 3); (4) mean stress vectors (σ_1 — maximum principal stress; σ_2 — intermediate principal stress; σ_3 — minimum principal stress) were calculated for each population by Bingham distribution statistics, and finally; (5) contour plots of fault orientations attributable to each stress tensor population were complied to illustrate the dominant fault geometry related to each deformation event (Fig. 4a–g). The veracity of each tensor population is indicated by eigenvalues, where a perfect concentration of *P*-axes (σ_1) and *T*-axes (σ_3) will be 0.5 and the intermediate axes (σ_2) will be zero (Allmendinger et al., 1992). The results of stress inversions are shown in Table 1.

3.2. Results

The development of *D*1 brittle–ductile high-strain zones and faults is attributable to northeast and southwest sub-horizontal contraction and sub-vertical extension (Fig. 3). The predominant fault geometries associated with this mean stress tensor are northwest-trending, moderately northeast- and southwest-dipping reverse faults (Fig. 4a). Fault transport was largely up–dip, however, left- and right-lateral components are evident on fault planes that are aligned obliquely to the maximum principal stress. Due to the inclusion of bedding–slip data associated with folding and thrusting of the Sodruzhestvo Group, a considerable spread of *P*-axes (eigenvalue = 0.2914) define the *D*1 stress tensor.

It has been suggested in a previous study that *D*2 structures formed during east–west to northwest–southeast directed extension (Läufer and Phillips, 2007). However, based on the differences in mean stress tensor and orientation of faults that formed during east–west and northwest–southeast directed extension, these data have been divided into two separate populations; the first characterised by east–west, sub-horizontal extension (*D*2) and the second by north-west–southeast sub-horizontal extension (*D*3).

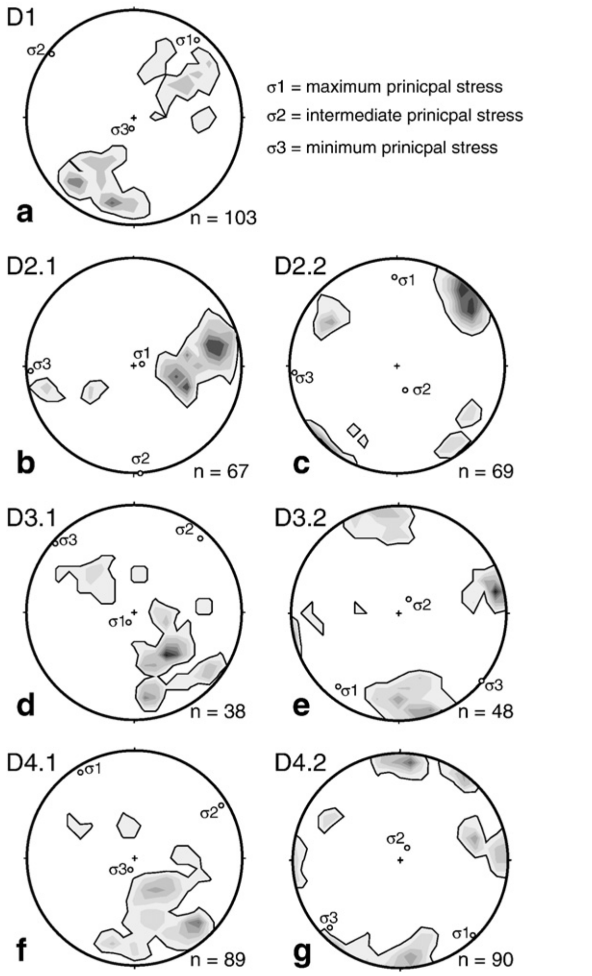

Fig. 4. Mean stress vectors (σ1 — maximum; σ2 — intermediate; σ3 — minimum) and the predominant fault geometries (as contoured poles) associated with each deformation event. (a) *D*1. (b–c) *D*2. (d–e) *D*3. (f–g) *D*4.

The first population (*D*2) is defined by east–west oriented, sub-horizontal *T*-axes (Figs. 3 and 4b–c). Of these data, sub-vertical (Fig. 4b) and north–south sub-horizontal *P*-axes are ubiquitous (Fig. 4c). Herein, faults that formed under this stress tensor are referred to as *D*2.1 and *D*2.2, respectively (Fig. 4b–c). Faults that formed during *D*2.1 are predominantly north-trending west- and east-dipping normal faults with west-dipping structures far more prevalent (Fig. 4b). In contrast, *D*2.2 faults trend northeast and southeast, are steeply dipping, and dominantly record evidence of right- and left-lateral normal transport (Fig. 4c). Based on similarities in *T*-axes orientation, we suggest that *D*2.1 and *D*2.2 structures are cogenetic.

The second population (*D*3) is defined by northwest–southeast oriented, sub-horizontal *T*-axes (Figs. 3 and 4d–e). Of these data, sub-vertical (Fig. 4d) and northwest–southeast sub-horizontal *P*-axes are evident (Fig. 4e). Throughout the remainder of the paper, faults that formed under these stress tensors are referred to as *D*3.1 and *D*3.2, respectively. *D*3.1 faults are dominantly northeast trending, dip to the northwest and show down–dip normal transport (Fig. 4d). Sub-horizontal northeast–southwest *P*-axes define *D*3.2 stress tensors, which resulted in the formation of north- and east-trending sub-vertical faults (Fig. 4e). As with the *D*2 structures, we suggest that due to the similarities in *T*-axes orientation, *D*3.1 and *D*3.2 structures formed cogenetically.

Overprinting relationships between mineral fibres on *D*2 faults support the division of *D*2 north–south from *D*3 northeast–southwest trending normal faults. Clear evidence for two phases of mineral fibre growth are preserved on *D*2 fault planes, where an earlier set aligned in a down–dip orientation (indicating normal transport) are generally overgrown by a second, obliquely oriented set (indicating right lateral transport). In addition to indicating that at least two phases of transport occurred along north–south trending *D*2 faults, this relationship proves that down–dip normal movement must have preceded right lateral-transport. Right lateral transport on north–south trending faults can be then explained by the reactivation of *D*2 normal faults by the *D*3 stress regime (Fig. 4b and d).

Two tensor populations are associated with late-stage *D*4 (*D*3 in the original deformation framework of Läufer and Phillips, 2007) brittle structures. Characteristic of both populations are relatively homogeneous *P*-axes defining sub-horizontal northwest–southeast oriented contraction (Fig. 3). The *D*4.1 tensor is characterised by sub-vertical *T*-axes that can be attributed to the reactivation of northeast-trending, northwest-dipping *D*3.1 normal faults (Fig. 4f). The *D*4.2 tensor is characterised by sub-horizontal southwest–northeast oriented extension that was associated with the reactivation of north- to east-trending *D*1 and *D*3.2 faults (Fig. 4g).

4. Discussion

4.1. The timing of tectonic deformation related to the evolution of the Lambert Graben

The timing of *D*1 to *D*4 events can be constrained by combining isotopic data, the timing of sediment deposition in East Antarctica and an understanding of global tectonics during the Carboniferous to Cretaceous. For *D*1, $^{40}Ar/^{39}Ar$ dating of white mica defining a shear fabric in a metre-wide *D*1 brittle–ductile high-strain zone yielded a plateau age of 491 ± 1 Ma and provides an absolute age of deformation (Phillips et al., 2007). In contrast, absolute dating of *D*2 and *D*3 structural features is yet to be attempted, and therefore, pre-existing geochronology, apatite fission track data and an understanding of the Phanerozoic depositional history of the Prince Charles Mountains–Prydz Bay region is employed to provide timing constraints. Whole rock and single mineral K-Ar dating indicate that the emplacement of felsic and mafic dykes in the Lambert Graben region during the Permian–Triassic (260–235 Ma) and early Cretaceous periods (140–100 Ma; Walker and Mond, 1971; Sheraton, 1983; Hofmann, 1991). Apatite fission track data indicate a similar scenario, where cooling associated with basement denudation

Table 1
Results of stress inversions.

	*D*1		*D*2.1		*D*2.2		*D*3.1		*D*3.2		*D*4.1		*D*4.2	
	Mean vector	Eigenvalue	Mean vector	Eigenvalue	Mean vector	Eigenvalue	Mean vector	Eigenvalue	Mean vector	Eigenvalue	Mean vector	Eigenvalue	Mean vector	Eigenvalue
σ_1	07 → 039	0.2914	84 → 078	0.3671	19 → 358	0.4155	81 → 208	0.3825	13 → 219	0.3908	06 → 328	0.3382	04 → 136	0.3332
σ_2	03 → 308	0.0749	01 → 177	0.0285	70 → 162	0.0086	09 → 042	0.0138	77 → 033	0.0121	07 → 059	0.0111	79 → 027	0.0606
σ_3	82 → 194	0.3663	06 → 267	0.3956	05 → 267	0.4241	02 → 311	0.3963	01 → 129	0.4028	81 → 197	0.3494	11 → 226	0.3938
n	103		67		69		38		48		89		90	

Statistically, principal stress axes calculated from a single population of data will have eigenvalues of 0.5 for σ1 and σ3 and 0.0 for σ2. Abbreviation: *n* — fault plane sample size comprising each palaeostress population.

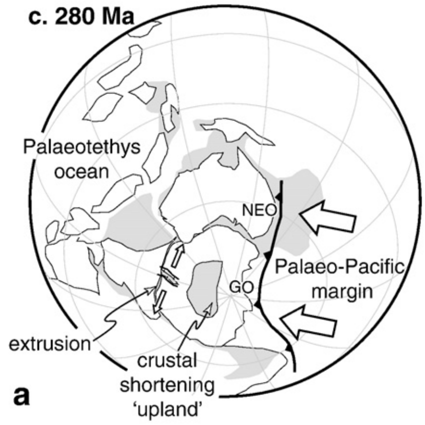

Fig. 5. Palaeogeographic reconstructions of East Gondwana at (a) 280 Ma and (b) 110 Ma. Enlargement shown in (b) illustrates overprinting relationships between *D*2 and *D*3 faults in the Lambert Graben region. Continental reconstructions are sourced from: (a) Geoscience Australia record GA07-1654 (doi: http://www.ga.gov.au/image_cache/GA100096.pdf); (b) Powell et al. (1988), Stagg et al. (2005).

occurred during the Carboniferous–Permian (350–300 Ma) and early Cretaceous periods (140–120 Ma; Arne, 1994; Lisker et al., 2003). Finally, sediment deposition can also be constrained to the Permian–Triassic and early Cretaceous by palynological data (Turner and Padley, 1991; McLoughlin and Drinnan, 1997a,b). It is also shown in this study that graben-forming events during *D*2 and *D*3 were associated with normal faulting and sub-horizontal crustal extension. Based on previous studies that have demonstrated a clear link between crustal extension, alkaline magmatism (Wilson and Downes, 1992), basement denudation (Lister and Davis, 1989) and sediment deposition, it is reasonable to constrain the timing of *D*2 and *D*3 extension to the Carboniferous–Permian and early Cretaceous time periods, respectively.

To test this new time-deformation framework, a comparison between palaeostress fields presented here and tectonic events in East Antarctica during the Carboniferous–Permian and Cretaceous is required. During the Carboniferous–Permian, East Antarctica was in a central position in eastern Gondwana (Fig. 5a). At this time, subduction along the Palaeo-Pacific margin was responsible for the development of the New England Orogen in eastern Australia and the Gondwanian Orogen in Antarctica (Fig. 5a; Leitch, 1974; Curtis et al., 2004; Glen, 2005). A passive margin associated with the opening of the Palaeotethys was also developing along the northern Gondwana margin at this time (Fig. 5a). A model for the intracratonic evolution of East Antarctica has been previously postulated by Veevers (1994), who attributed the development of an ancestral Gamburtsev upland to mid-Carboniferous crustal shortening from far field stress during the collision of Gondwana and Laurussia. Following this, Permian subsidence formed intracratonic basins throughout Gondwana. Lisker et al. (2003) expanded on this hypothesis and suggested that convergent margin tectonics along the Palaeo-Pacific margin was probably responsible for crustal thickening in central Antarctica and extrusion behind the upland (Fig. 5a). To further explore the likelihood of this model, the Baikal Rift, the Tibetan Plateau and the India–Eurasia collision potentially provide a modern analogy.

Located to the north of the Tibetan Plateau, the Baikal Rift is aligned approximately normal to the India–Eurasian collision zone (Fig. 6; Artyushkov et al., 1991; Zorin and Cordell, 1991). The rift zone formed during Oligocene to Recent times and developed coevally with the India–Eurasia collision. Based on this temporal link, it has been previously suggested that crustal extension was caused by tectonic extrusion and is a distal response (~3000 km) to the India–Eurasia collision (Molnar and Tapponier, 1975). As previously mentioned, a similar model is proposed for East Antarctica, where Lisker et al. (2003) suggested that convergence along the Palaeo-Pacific margin was responsible for a central upland and extrusion tectonics in the Lambert Graben region. Conversely, physical modelling of deformation behind the Tibetan Plateau has shown that the Baikal Rift probably formed by extension driven by slab-rollback along the rift-parallel Kuril subduction system (Fig. 6; Schellart and Lister, 2005). This creates significant doubt in the effectiveness of plate margin convergence to drive intracontinental extrusion at large distances. Nevertheless, as an active convergent margin did not exist parallel to the Lambert Graben during Permian times (Fig. 5a), as with the current relationship between the Baikal Rift and Kuril subduction system, the Permian extrusion model for intracontinental deformation in East Antarctica cannot be precluded. Owing to this major difference between the India–Eurasian collision–Baikal Rift and Palaeo-Pacific margin–Lambert Graben systems, we support the

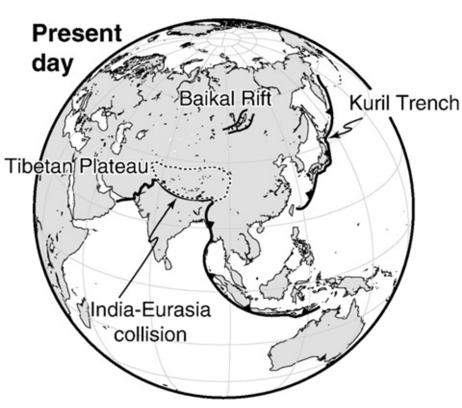

Fig. 6. Map showing the geographic positions of the India–Eurasia collision, Tibetan Plateau, Baikal Rift and Kuril subduction system for comparison with the tectonic state of East Antarctica during the Permian (shown in Fig. 5a). Map constructed using Generic Mapping Tools version 4.3.1 (Wessel and Smith, 1998).

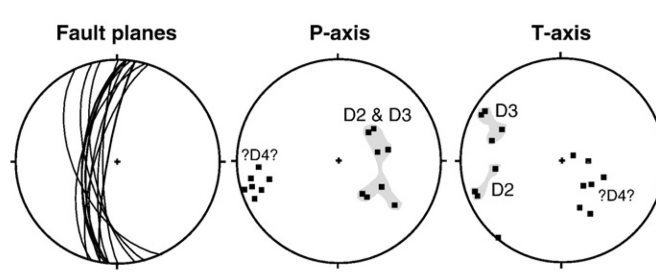

Fig. 7. Kinematic data collected in the northern Prince Charles Mountains by Boger and Wilson (2003). Fault plane orientation, *P*- and *T*-axes of faults measured from Radok Lake (Fig. 2), northern Prince Charles Mountains.

model of Lisker et al. (2003) and advocate that extrusion provides the most likely mechanism to explain Carboniferous-Permian continental extension in the Lambert Graben region of East Antarctica.

Volcanic activity in central East Gondwana increased during the early Cretaceous period, which has been suggested to represent the arrival of the Kerguelen plume (Frey et al., 2000). The arrival of this plume led to extensive plume-related magmatism in Antarctica, Australia and India, and has been attributed to the eventual break-up of East Gondwana at 130–100 Ma (Fig. 5b; Powell et al., 1988; Frey et al., 1996; Yang et al., 1998; Coffin et al., 2002). Relative plate motions associated with the break-up of East Gondwana are constrained by sea-floor spreading isochrones, which indicate northwest–southeast directed transport between India and East Antarctica (Powell et al., 1988; Gaina et al., 2007). A comparable palaeostress field is calculated for the *D*3 evolution of the Lambert Graben in this study. Based on this correlation, we suggest that the compartmentalisation of the north–south oriented graben architecture by northwest-trending normal faults is attributed to the early Cretaceous break-up of India and Antarctica (Fig. 5b).

Boger and Wilson (2003) present an alternate scenario to the model presented in this study. They suggest that the Lambert Graben formed as a broad transtensional basin during the early Cretaceous break-up of East Gondwana. This assumption was based on the inversion of a small kinematic dataset that resulted in the calculation of a single palaeostress field characterised by northwest–southeast directed sub-horizontal extension. As this direction of extension was largely parallel to that suggested during the break-up of India and Antarctica (Powell et al., 1988), the timing of brittle deformation in the Prince Charles Mountains was also inferred to be entirely Cretaceous in age (Boger and Wilson, 2003). To test the compatibility of the present study with that of Boger and Wilson (2003), we performed stress inversions on kinematic data collected during a reconnaissance

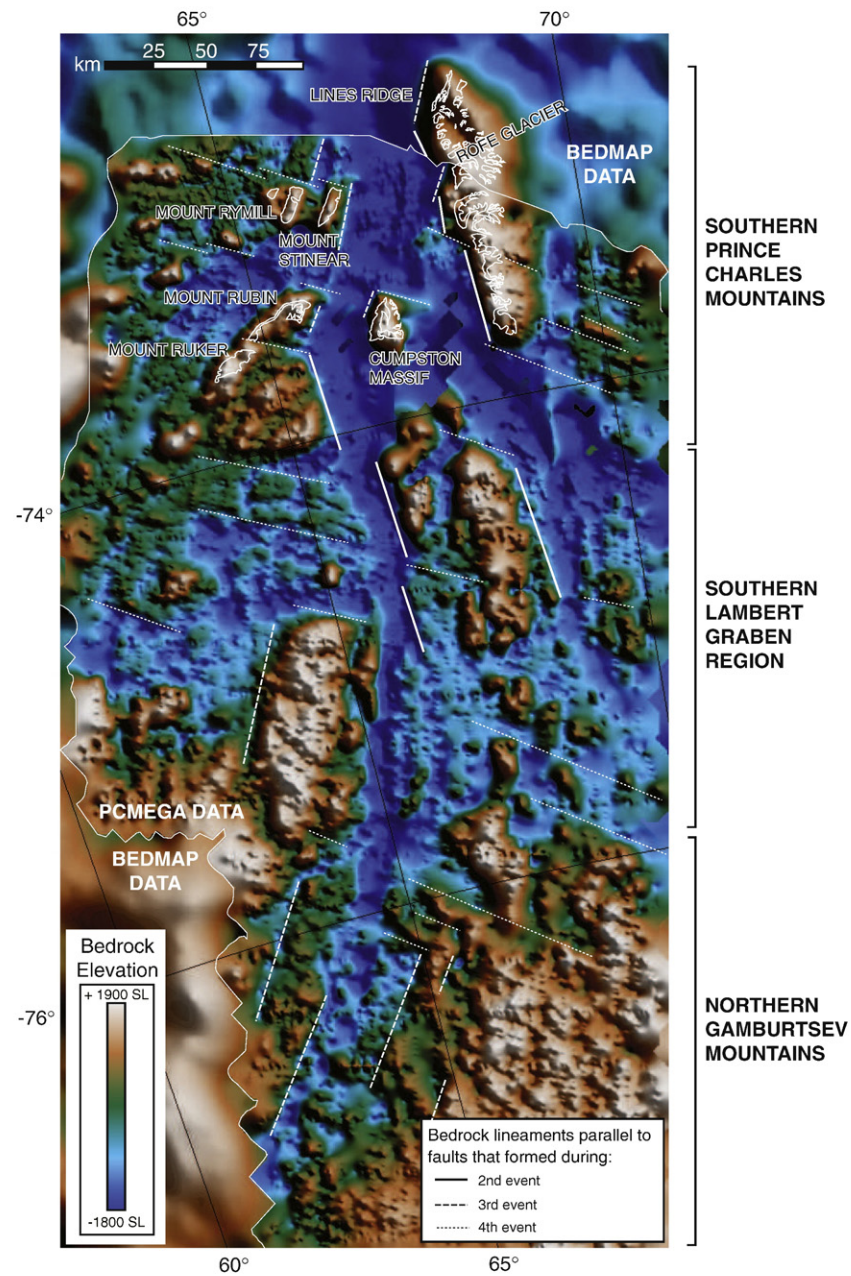

Fig. 8. Ice-radar data showing sub-ice topography in the southern Prince Charles Mountains, southern Lambert Glacier region and northern Gamburtsev Mountains. Topography is predominantly defined by north-trending, northeast-trending and east–southeast trending lineaments. Low-resolution sub-ice bedrock data is from the BEDMAP database (Lythe et al., 2000); high-resolution sub-ice bedrock data is from the PCMEGA database (Damm, 2007).

study from the northern Prince Charles Mountains (Table 1 of Boger and Wilson, 2003). The reappraisal of these data resulted in the identification of clear similarities with the dataset presented in this study. Firstly, faults located in the northern Prince Charles Mountains predominantly strike north–south, which are comparable in orientation to graben parallel *D*2 faults identified in this study (Fig. 7). Secondly, calculated *P*–*T* axes are similar to the *D*2 and *D*3 stress tensors calculated in the present study. For example, kinematic data show clear evidence for east–west oriented, sub-horizontal extension, that is comparable to the *D*2 stress tensor calculated here. Furthermore, *P*–*T* axes indicating northwest–southeast sub-horizontal extension comparable to the *D*3 stress tensor are also evident (Fig. 7). There is also evidence that reactivation (*D*4) of north–south trending *D*2 structures probably occurred (Fig. 7). Combined, these data clearly indicate a poly-stage structural evolution for the Lambert Graben, which is in agreement with the deformation framework presented in the current study.

4.2. Geomorphologic induced deformation in the Lambert Graben region

In contrast to the *D*1–*D*3 events described in this paper, the absolute timing of *D*4 is difficult to constrain. Firstly, there is no evidence for burial or exhumation (heating or cooling) in the low-temperature thermochronological record after the Cretaceous (Arne, 1994; Lisker et al., 2003, 2007). This indicates that *D*4 must have occurred at temperatures below the annealing of apatite fission tracks (<60°) and, therefore, in the upper 2–3 km of the crust; assuming a geothermal gradient of 20–30 °C/km. Secondly, the *D*4 palaeostress tensor is not comparable to known far-field tectonic stress regimes that affected the Antarctic plate after the Cretaceous period. Thirdly, the only preserved sedimentary rocks deposited after Cretaceous times are the Pagodroma Group, which is interpreted to represent glaciomarine sediments attributed to glacial erosion (McKelvey et al., 2001). Finally, the only reliable evidence for magmatism is the eruption of tephritic phonolite lava at 50 ± 2 Ma (Sheraton, 1983). Based on these lines of evidence, support for tectonically driven deformation in the Lambert Graben region after the Cretaceous is significantly lacking.

Glaciation of Antarctica during the late Eocene (Kennett, 1977) would have resulted in a considerable isostatic response due to crustal loading. Models of bedrock uplift relative to ice-sheet retreat or advance demonstrate a clear relationship between changes in ice volume and isostasy of the underlying crust (Zwartz et al., 1998). Expanding on this idea, Stern et al. (2005) demonstrated that selective glacial erosion could result in a localised isostatic response that would contribute to an increase in vertical plate velocity. Based on a loading-flexural model of the isostatic response to glacial incision, Stern et al. (2005) showed that selective erosion could be the cause of up to 50% (~2000 m) of the peak elevation of the Transantarctic Mountains. This may also be true for the Lambert Graben region, where localised erosion by the Lambert Glacier could result in significant crustal unloading and a local isostatic response. This response would manifest as an acceleration in vertical plate velocity, and thus provide a potential cause for fault reactivation during *D*4.

4.3. On the relationship between inherited tectonic structure and landscape evolution

Radio-echo ice-radar studies in the southern Prince Charles Mountains–Gamburtsev Mountains region of East Antarctica provide data that allows the bedrock topography to be delineated (Fig. 8). The most prominent topographic feature in the southern Prince Charles Mountains is the Mawson Escarpment, which is bound on its western side by north-oriented lineaments that represent approximately ~2200 m of relief. Lineaments of comparable orientation bound the eastern sub-ice margin of Mount Ruker (Fig. 8). Northeast-trending linear features truncate the dominant north-trending escarpments (Fig. 8). Examples of these lineaments are preserved south of the Rofe Glacier, the eastern margin of Mount Stinear and Mount Rubin and the northwestern margin of Cumpston Massif (Fig. 8). The northern margin of the Mawson Escarpment (Lines Ridge), even though not defined by the high-resolution ice-radar data, is also defined by a linear outcrop pattern defined by this northeasterly strike.

A third set of lineaments that consistently trend east–southeast define the northern margin of Mounts Stinear and Rymill, the northern margin of Cumpston Massif and Mount Rubin, as well as delineating tributary glaciers located along the southern Mawson Escarpment and between Mount Rubin and Ruker (Fig. 8). Many predominant sub-ice features are also characterised by this east–southeast orientation, which is particularly evident along the eastern margin and northwestern corner of the ice-radar image. Furthermore, evidence for offset of north- and northeast-trending escarpments along these lineaments is preserved along the eastern margin of Mount Rubin, the northeastern margin of Cumpston Massif and to the south of the Rofe Glacier along the Mawson Escarpment. Based on these relations, the east-southeast trending lineaments are interpreted to represent the youngest bedrock geomorphological features in the southern Prince Charles Mountains.

It is currently unclear whether the described bedrock lineaments are related to tectonic or geomorphological processes. If they were tectonic in nature, it would be reasonable to argue that the current landscape in the Lambert region is defined by tectonic structures of Permian- or Cretaceous-age, and is therefore, an extremely long-lived landscape. On the other hand, it is suggested that a planation surface that defines the tops of nunataks in the southern Prince Charles Mountains reflects a once contiguous fluvial erosion surface (Bardin, 1977). If incision into and erosion of this palaeosurface commenced after the Oligocene glaciation of Antarctica, the effectiveness of glacial incision and its relation to erosion controlled uplift since the Miocene can be evaluated (Stern et al., 2005; Hambrey et al., 2007).

The Cenozoic history of the Prince Charles Mountains is characterised by glaciation, uplift and erosion. Evidence for uplift is based on the present-day altitude (~1500 masl) of glaciomarine sedimentary units of the Pagodroma Group, which are based on knowledge of sea level variations since their deposition, cannot be attributable to changes in eustasy (Miller et al., 1998). A lack of neotectonic faults preserved in the Pagodroma Group also indicates that recent tectonic activity was probably not the cause of uplift (McKelvey et al., 2001). Instead, we suggest that uplift was related to local crustal unloading and plate flexure. A study of sediment back stacking onto the present-day landscape supports this, where it has been shown that mass erosion during the Cenozoic was dominantly localised in the Lambert Graben region (Jamieson et al., 2005). Intensive erosion would result in maximum crustal unloading in the Lambert region, and therefore, the greatest isostatic response.

To explain the present-day landscape in the Lambert Graben region, we propose a model where both tectonic and geomorphologic processes were responsible. Based on the striking similarities between bedrock lineaments and the brittle deformation record, we argue that the incipient development of these lineaments was tectonic and probably related to the Carboniferous–Cretaceous tectonic evolution of the Lambert Graben. As topography in the region is also defined by these lineaments, we propose that the uplift be driven by an isostatic response to intensive, localised crustal unloading and plate flexure. Uplift was then accommodated by the inherited brittle architecture of the ancient Lambert Graben. Similar models are invoked to explain the evolution of modern orogenic systems, where inherited structures are suggested to play an integral role in defining the architecture of an orogen (Williams et al., 1989; Butler et al., 2006). The model proposed here expands on this by highlighting the potential importance that inherited tectonic structures may also have in controlling landscape evolution in regions of dynamic isostasy, which, in this case, was driven by geomorphologic processes.

4.4. Evolution of the sub-glacial Gamburtsev Mountains

Based on the hypothesis proposed for the development of relief in the southern Prince Charles Mountains, we attempt to explain the evolution of the present-day sub-glacial Gamburtsev Mountains (Fig. 2). In the context of the current hypothesis, the Gamburtsev Mountains probably formed via a two-stage process: (1) tectonic events of Carboniferous–Permian and Cretaceous age responsible for brittle fracturing of the lithosphere, and (2) geomorphologic forcing responsible for dynamic isostasy, some fault reactivation and uplift.

Lineaments characterising the southern Lambert Graben and northern Gamburtsev Mountains show remarkable similarities to those identified in the southern Prince Charles Mountains. In the southern Lambert Graben region, predominant north-trending lineaments can be traced from the southern Mawson Escarpment down to the Gamburtsev Mountains where they are truncated by the east–southeast oriented front of the range (Fig. 8). This is a consistent relation seen to the north of the Gamburtsev Mountains, where positive topography defined by north-trending lineaments are cut by northeast-trending and east–southeast oriented lineaments that compartmentalise the topography into a series of sub-ice ranges and valleys (Fig. 8). Small escarpments and basins that trend northeast characterise the western margin of the Gamburtsev Mountains. These bedrock features are in a comparable orientation to the eastern margins of Mounts Stinear and Rubin and the northern margin of the Mawson Escarpment (Fig. 8). In contrast, east–northeast trending escarpments define the northern margin, as well as peaks and valleys that define the interior topography of the Gamburtsev mountain range. These east–southeast oriented lineaments are also conspicuous throughout the southern Lambert Graben and Prince Charles Mountains. Based on the previously made assumption that bedrock lineaments parallel ancient fault zones, it is clear that a strong spatial link also exists between the orientations of the $D2$–$D4$ fault arrays identified in the southern Prince Charles Mountains and bedrock lineaments identified in the southern Lambert Graben–northern Gamburtsev Mountains region.

Assuming that the escarpments defining the northern and western range fronts of the Gamburtsev Mountains represent ancient fault zones, it can then be suggested that the Gamburtsev Mountains are bound by a bifurcation of the Lambert Rift system (Fig. 8). A modern example of rift bifurcation is the divergence of the East African Rift around the tectonically rigid Tanzania shield (Nyblade and Brazier, 2002), where bifurcation is related to the pre-rift rheology of the lithosphere. Using this as an analogy, we suggest that the Gamburtsev Mountains could represent a rigid lithospheric block that is surrounded by lithosphere of considerably reduced strength. This is supported by the palaeogeographic reconstructions of Antarctica in Veevers and Saeed (2008), where East Antarctica comprises a collage of rigid Archaean–Palaeoproterozoic cratons embedded in a matrix of younger, and presumably weaker, orogenic belts. Based on these assumptions, we suggest that the initial origins of the Gamburtsev Mountains may be related to incipient brittle deformation relating to the development of the Lambert Graben, and therefore, be mid-Carboniferous to Permian in age (Veevers, 1994). Uplift relating to the present-day relief is, however, argued to be a much younger feature. Localised erosion and crustal unloading along the Lambert Graben can explain this. The isostatic rebound associated with crustal unloading increased vertical velocity of the plate, which was translated into uplift. Uplift could then be accommodated by fractures in the lithosphere that were inherited from ancient tectonic events.

5. Conclusion

This study has identified at least four stages of ductile–brittle to brittle deformation in the Lambert Graben region of East Antarctica. In combination with pre-existing sedimentological, geochronological and palaeogeographical studies, this deformation framework allows a comprehensive model for intracontinental deformation in East Antarctica to be elucidated. Based on new palaeostress constraints presented here, we suggest that the initial formation of the Lambert Graben was the result of pure extension during Carboniferous–Permian times. Extension was probably driven by intracontinental extrusion related to convergent plate margin processes along the Palaeo-Pacific margin. Following this, compartmentalisation of the graben by northwest trending normal faults was driven by transtension associated with the early Cretaceous break-up of India and East Antarctica. The most recent deformation event was predominantly associated with reactivation of pre-existing faults that was probably caused by dynamic isostasy in the region.

The brittle deformation architecture in the southern Prince Charles Mountains also provides inferences on the development of relief in a glaciated region. If it can be shown that intensive erosion along the Lambert Graben during the Cenozoic caused localised unloading, plate flexure and uplift, it would be reasonable to argue that relief development in the Prince Charles Mountains was accommodated by inherited Carboniferous–Permian and early Cretaceous brittle tectonic structures. This being the case, we suggest that a combination of tectonic and geomorphologic processes were responsible for the development of relief in the Lambert Graben region of East Antarctica.

Acknowledgements

The Australian Antarctic Division (AAS Grant 1215) and the Bundesanstalt für Geowissenschaften und Rohstoffe (BGR) are thanked for logistical and financial support of the 2002–03 PCMEGA field season in Antarctica. G.P. acknowledges the support of a Scientific Committee of Antarctic Research Fellowship. A.L. thanks BGR for invitation on to the PCMEGA expedition and acknowledges Deutsche Forschungsgemeinschaft (DFG) for financial support (Grant LA 1080/4-1). Thanks to Mark McLean for providing bedrock elevation maps and Chris Wilson for assistance in the field. Frank Lisker and Robin Offler provided comments on an earlier version of the manuscript and John Veevers provided an official review.

References

Allmendinger, R.W., Marrett, R.A., Cladouhos, T., 1992. Faultkin, A Computer Program for Analysis of Fault Slip Data.
Andronikov, A.V., Foley, S.F., Beliatsky, B.V., 1998. Sm-Nd and Rb-Sr isotopic systematics of the East Antarctic Manning Massif alkaline trachybasalts and the development of the mantle beneath the Lambert–Amery rift. Mineralogy and Petrology 63, 243–261.
Angelier, J., 1979. Determination of the mean principal stresses for a given fault population. Tectonophysics 56, T17–T26.
Angelier, J., Mechler, P., 1977. Sur une méthode graphique de recherche des contraintes principales égalment utilisable en tectonique et en seismologie: La méthode des dièdres droits. Bulletin Société Géologique de France 19, 1309–1318.
Arne, D.C., 1994. Phanerozoic exhumation history of the northern Prince Charles Mountains (East Antarctica). Antarctic Science 6, 69–84.
Artyushkov, E.V., Baer, M.A., Letnilov, F.A., Ruzhich, V.V., 1991. On the mechanism of graben formation. Tectonophysics 197, 99–115.
Bardin, V.I., 1977. Glacial geomorphology of the Lambert Glacier and the surrounding mountain area. Polar Geography 1, 251–269.
Boger, S.D., Wilson, C.J.L., 2003. Brittle faulting in the Prince Charles Mountains, East Antarctica: Cretaceous transtensional tectonics related to the break-up of Gondwana. Tectonophysics 367, 173–186.
Boger, S.D., Wilson, C.J.L., Fanning, C.M., 2006. An Archaean province in the southern Prince Charles Mountains, East Antarctica: U-Pb zircon evidence for c. 3170 Ma granite plutonism and c. 2780 Ma partial melting and orogenesis. Precambrian Research 145, 307–328.
Boger, S.D., Maas, R., Fanning, C.M., 2008. Isotopic and geochemical constraints on the age and origin of granitoids from the central Mawson Escarpment, southern Prince Charles Mountains, East Antarctica. Contributions to Mineralogy and Petrology 155, 379–400.

Butler, R.W.H., Tavarnelli, E., Grasso, M., 2006. Structural inheritance in mountain belts: an Alpine–Apennine perspective. Journal of Structural Geology 28, 1893–1908.

Coffin, M.F., Pringle, M.S., Duncan, R.A., Gladczenko, T.P., Storey, M., Müller, R.D., Gahagan, L.A., 2002. Kerguelen hotspot magma output since 130 Ma. Journal of Petrology 43, 1121–1137.

Corvino, A.F., Boger, S.D., Wilson, C.J.L., 2007. *P–T* conditions during formation of a metapelitic gneiss from Clemence Massif, Antarctic Prince Charles Mountains. In: Cooper, A., et al. (Ed.), A Keystone in a Changing World — Online Proceedings for the 10th International Symposium on Antarctic Earth Sciences. U.S. Geological Survey Open-File Report 2007-1047. doi:10.3133/of2007-1047.srp062.

Corvino, A.F., Boger, S.D., Henjes-Kunst, F., Wilson, C.J.L., Fitzsimons, I.C.W., 2008. Superimposed tectonic events at 2450 Ma, 2100 Ma, 900 Ma and 500 Ma in the North Mawson Escarpment, Antarctic Prince Charles Mountains. Precambrian Research 167, 281–302.

Curtis, M.L., Millar, I.L., Storey, B.C., Fanning, M., 2004. Structural and geochronological constraints of early Ross orogenic deformation in the Pensacola Mountains, Antarctica. GSA Bulletin 116, 619–636.

Damm, V., 2007. A subglacial topographic model of the southern drainage area of the Lambert/Glacier/Amery Ice Shelf System — results of an airborne ice thickness survey south of the Prince Charles Mountains. Terra Antartica 14, 85–94.

Federov, L.V., Ravich, M.G., Hofmann, J., 1982. Geological comparison of southeastern peninsular India and Sri Lanka with a part of East Antarctica (Enderby Land, MacRobertson Land, and Princess Elizabeth Land). In: Craddock, C. (Ed.), Antarctic Geology and Geophysics. University of Wisconsin Press, Madison, pp. 73–78.

Frey, F.A., McNaughton, N.J., Nelson, D.R., deLaeter, J.R., Duncan, R.A., 1996. Petrogenesis of the Bunbury Basalt, Western Australia: interaction between the Kerguelen plume and Gondwana lithosphere? Earth and Planetary Science Letters 144, 163–183.

Frey, F.A., Coffin, M.F., Wallace, P.J., Weis, D., Zhao, X., Wise Jr., S.W., Wahnert, V., Teagle, D.A.H., Saccocia, P.J., Reusch, D.N., Pringle, M.S., Nicolaysen, K.E., Neal, C.R., Müller, R.D., Moore, R.D., Mahoney, C.L.J.J., Keszthelyi, L., Inokuchi, H., Duncan, R.A., Delius, H., Damuth, J.E., Damasceno, D., Coxall, H.K., Borre, M.K., Boehm, F., Barling, J., Arndt, N.T., Antretter, M., 2000. Origin and evolution of a submarine large igneous province: the Kerguelen Plateau and Broken Ridge, southern Indian Ocean. Earth and Planetary Science Letters 176, 73–89.

Gaina, C., Müller, R.D., Brown, B., Ishihara, T., Ivanov, S., 2007. Breakup and early seafloor spreading between India and Antarctica. Geophysical Journal International 170, 151–169.

Geoscience Australia record GA07-1654. doi: http://www.ga.gov.au/image_cache/GA100096.pdf.

Glen, R.A., 2005. The Tasmanides of eastern Australia. In: Vaughan, A.P.M., Leat, P.T. (Eds.), Terrane Processes at the Margins of Gondwana. Special Publication — Geological Society of London, vol. 246. London, pp. 23–96.

Hambrey, M.J., Glasser, N.F., McKelvey, B.C., Sugden, D.E., Fink, D., 2007. Cenozoic landscape evolution of an East Antarctic oasis (Radok Lake area, northern Prince Charles Mountains), and its implications for the glacial and climatic history of Antarctica. Quaternary Science Reviews 26, 598–626.

Harrowfield, M., Holdgate, G., Wilson, C.J.L., McLoughlin, S., 2005. Tectonic significance of the Lambert Graben, East Antarctica: reconstructing the Gondwanan rift. Geology 33, 197–200.

Hofmann, J., 1991. Fault tectonics and magmatic ages in the Jetty Oasis area, MacRoberston Land: a contribution to the Lambert rift development. In: Thomson, M.R.A., et al. (Ed.), The Geological Evolution of Antarctica. Cambridge University Press, pp. 107–112.

Jamieson, S.S.R., Hulton, N.R.L., Sugden, D.E., Payne, A.J., Taylor, J., 2005. Cenozoic landscape evolution of the Lambert basin, East Antarctica: the relative role of rivers and ice sheets. Global and Planetary Change 45, 35–49.

Kamenev, E.N., Andronikov, A.V., Mikhalsky, E.V., Krasnikov, N.N., Stüwe, K., 1993. Soviet geological maps of the Prince Charles Mountains, East Antarctic Shield. Australian Journal of Earth Sciences 40, 501–517.

Kennett, J.P., 1977. Cenozoic evolution of Antarctic glaciation, the circum-Antarctic Ocean, and their impact on global Palaeoceanography. Journal of Geophysical Research 82, 3843–3860.

Läufer, A.L., Phillips, G., 2007. Brittle deformation events in the Lambert Glacier region (East Antarctica): insights into the tectonic control on the formation and evolution of the Lambert Graben. Terra Antartica 14, 61–68.

Leitch, E.C., 1974. The geological development of the southern part of the New England Fold Belt. Australian Journal of Earth Sciences 21, 133–156.

Lisker, F., Brown, R., Fabel, D., 2003. Denudation and thermal history along a transect across the Lambert Graben, northern Prince Charles Mountains, Antarctica, derived from apatite fission track thermochronology. Tectonics 22. doi:10.1029/2002TC001477.

Lisker, F., Gibson, H., Wilson, C.J., Läufer, A.L., 2007. Denudation and uplift of the Mawson Escarpment (eastern Lambert Graben, Antarctica) as indicated by apatite fission track data and geomorphological observation. In: Cooper, A., et al. (Ed.), A Keystone in a Changing World-Online Proceedings for the 10th International Symposium on Antarctic Earth Sciences. U.S. Geological Survey Open-File Report 2007-1047. doi:10.3133/of2007-1047.srp105.

Lister, G.S., Davis, G.A., 1989. The origin of metamorphic core complexes and detachment faults formed during Tertiary continental extension in the northern Colorado River region, U.S.A. Journal of Structural Geology 11, 65–94.

Lythe, M.B., Vaughan, D.G. and the BEDMAP Consortium, 2000. BEDMAP — Bed Topography of the Antarctic 1:100,000,000 Scale Map. British Antarctic Survey (Misc) 9. Cambridge, British Antarctic Survey.

Marrett, R., Allmendinger, R.W., 1990. Kinematic analysis of fault-slip data. Journal of Structural Geology 12, 973–986.

McLean, M.A., Rawling, T.J., Betts, P.G., Phillips, G., Wilson, C.J.L., 2008. Three-dimensional inversion modelling of a Neoproterozoic basin in the southern Prince Charles Mountains, East Antarctica. Tectonophysics 456, 180–193.

McKelvey, B.C., Hambrey, M.J., Harwood, D.M., Mabin, M.C.G., Webb, P.-N., Whitehead, J.M., 2001. The Pagodroma Group — a Cenozoic record of the East Antarctica ice sheet in the northern Prince Charles Mountains. Antarctic Science 13, 455–468.

McLoughlin, S., Drinnan, A.N., 1997a. Revised stratigraphy of the Permian Bainmedart coal measures, northern Prince Charles Mountains, East Antarctica. Geological Magazine 134, 335–353.

McLoughlin, S., Drinnan, A.N., 1997b. Fluvial sedimentology and revised stratigraphy of the Triassic Flagstone Bench Formation, northern Prince Charles Mountains, East Antarctica. Geological Magazine 134, 781–806.

Mikhalsky, E.V., Sheraton, J.W., Labia, A.A., Tingey, R.J., Thost, D.E., Kamenev, E.N., Fedorov, L.V., 2001. Geology of the Prince Charles Mountain, Antarctica. AGSO Bulletin 247.

Miller, K.G., Mountains, G.S., Browning, J.V., Kominz, M., Sugarman, P.J., Christie-Blick, N., Katz, M.E., Wright, J.D., 1998. Cenozoic global sea level sequences, and the New Jersey transect: results from coastal plain and continental slope drilling. Reviews of Geophysics 36, 569–601.

Mishra, D.C., Chandra Sekhar, D.V., Venkata Raju, D.Ch., Vijaya Kumar, V., 1999. Crustal structure based on gravity–magnetic modelling constrained from seismic studies under Lambert Rift, Antarctica and Godavari and Mahanadi rifts, India and their interrelationship. Earth and Planetary Science Letters 172, 287–300.

Molnar, P., Tapponier, P., 1975. Cenozoic tectonics of Asia: effects of a continental collision: features of recent continental tectonics in Asia can be interpreted as a result of the India–Eurasia collision. Science 8, 419–426.

Nyblade, A.A., Brazier, R.A., 2002. Precambrian lithospheric controls on the development of the East African rift system. Geology 30, 755–758.

Phillips, G., 2007. The Tectonic History of the Ruker Province, Southern Prince Charles Mountains, East Antarctica: Implications for Gondwana and Rodinia. Unpublished PhD Thesis, The University of Melbourne.

Phillips, G., Wilson, C.J.L., Campbell, I.H., Allen, C.M., 2006. U-Th-Pb detrital geochronology from the southern Prince Charles Mountains, East Antarctica — defining the Archaean to Neoproterozoic Ruker Province. Precambrian Research 148, 292–306.

Phillips, G., Wilson, C.J.L., Phillips, D., Szczepanski, S.K., 2007. Early Palaeozoic basin inversion within the southern Prince Charles Mountains, East Antarctica: implications of the construction of Gondwana. Journal of the Geological Society of London 164, 771–784.

Powell, C.McA, Roots, S.R., Veevers, J.J., 1988. Pre-breakup continental extension in east Gondwanaland and the early opening of the eastern Indian Ocean. Tectonophysics 155, 19–40.

Schellart, W.P., Lister, G.S., 2005. The role of the East Asian active margin in widespread extensional and strike–slip deformation in East Asia. Journal of the Geological Society 162, 959–972.

Sheraton, J.W., 1983. Geochemistry of mafic igneous rocks of the northern Prince Charles Mountains. Journal of the Geological Society of Australia 30, 295–304.

Stagg, H.M.J., Colwell, J.B., Direen, N.G., O'Brien, P.E., Brown, B.J., Bernardel, G., Borissova, I., Carson, L., Close, D.B., 2005. Geological framework of the continental margin in the region of the Australian Antarctic Territory. Geoscience Australia Record 2004/25.

Stern, T.A., Baxter, A.K., Barrett, P.J., 2005. Isostatic rebound due to glacial erosion within the Transantarctic Mountains. Geology 33, 221–224.

Tewari, R.C., Veevers, J.J., 1993. Gondwana basins of India occupy the middle of a 7500 km sector of radial valleys and lobes in central–eastern Gondwanaland. In: Findlay, R.H., et al. (Ed.), Gondwana Eight. Balkema, Rotterdam, pp. 507–512.

Tingey, R.J., 1991. The regional geology of Archaean and Proterozoic rocks in Antarctica. In: Tingey, R.J., et al. (Ed.), The Geology of Antarctica. Oxford University Press, Great Britain, pp. 1–73.

Turner, F.J., 1953. Nature and dynamic interpretation of deformation lamellae in calcite of three marbles. American Journal of Science 251, 276–298.

Turner, B.R., Padley, D., 1991. Lower Cretaceous coal-bearing sediments from Prydz Bay, East Antarctica. In: Barron, J., Larsen, B., et al. (Eds.), Proc. ODP, Science Results, vol. 119. Ocean Drilling Program, College Station, TX, pp. 57–60.

Veevers, J.J., 1994. Case for the Gamburtsev subglacial mountains of East Antarctica originating by mid-Carboniferous shortening of an intracratonic basin. Geology 22, 593–596.

Veevers, J.J., Saeed, A., 2008. Gamburtsev Subglacial Mountains provenance of Permian–Triassic sandstones in the Prince Charles Mountains and offshore Prydz Bay: integrated U-Pb and TDM ages and host-rock affinity from detrital zircons. Gondwana Research 14, 316–342.

Walker, K.R., Mond, A., 1971. Mica lamprophyre (alnöite) from Radock Lake, Prince Charles Mountains, Antarctica. Australian Bureau of Mineral Resources Record 1971/108, p. 6.

Wellman, P., Tingey, R.J., 1981. Glaciation, erosion and uplift over part of East Antarctica. Nature 291, 142–144.

Wessel, P., Smith, W.H.F., 1998. New, improved version of Generic Mapping Tools released. EOS Transactions American Geophysics Union 79 (47), 579.

Williams, G.D., Powell, C.M., Cooper, M.A., 1989. Geometry and kinematics of inversion tectonics. In: Cooper, M.A., Williams, D.G. (Eds.), Inversion Tectonics. Special Publication-Geological Society of London, vol. 44, pp. 3–15.

Wilson, M., Downes, H., 1992. Mafic alkaline magmatism associated with the European Cenozoic rift system. Tectonophysics 208, 173–182.

Yang, H.-J., Frey, F.A., Weis, D., Giret, A., Pyle, D., Michon, G., 1998. Petrogenesis of the flood basalts forming the northern Kerguelen Archipelago: implications for the Kerguelen Plume. Journal of Petrology 39, 711–748.

Zorin, Yu.A., Cordell, L., 1991. Crustal extension in the Baikal rift zone. Tectonophysics 198, 117–121.

Zwartz, D., Bird, M., Stone, J., Lambeck, K., 1998. Holocene sea-level change and ice-sheet history in the Vestfold Hills, East Antarctica. Earth and Planetary Science Letters 155, 131–145.